Polymer 49 (2008) 4420–4426

Contents lists available at ScienceDirect

Polymer

journal homepage: www.elsevier.com/locate/polymer

Effect of copolymer compositions on the miscibility behavior and specific interactions of poly(styrene-*co*-vinyl phenol)/poly(vinyl phenyl ketone) blends

Shiao Wei Kuo*

Department of Materials and Optoelectronic Science, Center for Nanoscience and Nanotechnology, National Sun Yat-Sen University, Kaohsiung, 804, Taiwan

ARTICLE INFO

Article history:
Received 7 May 2008
Received in revised form 30 July 2008
Accepted 4 August 2008
Available online 7 August 2008

Keywords:
Copolymer blend
Hydrogen bonding
π–π interaction

ABSTRACT

Differential scanning calorimetry and one- and two-dimensional Fourier transform infrared (FTIR) spectroscopies have been used to investigate the miscibility of and specific interactions between poly(styrene-*co*-vinyl phenol) (PSOH) and poly(vinyl phenyl ketone) (PVPK) upon varying the vinyl phenol content of the PSOH copolymer. The FTIR spectra revealed that the phenol units of PVPh interact strongly with the C=O groups of PVPK through intermolecular hydrogen bonding, and more weakly with the aromatic rings of PVPK through intermolecular π–π interactions. A miscibility window exists when the vinyl phenol fraction in the copolymer is greater than 20 mol% in the PSOH/PVPK blend system, as predicted using the Painter–Coleman association model.

1. Introduction

One approach toward preparing new materials exhibiting tunable properties is the blending of two or more polymers [1]. Unfortunately, most polymer blends are immiscible because of their high degrees of polymerization; as a result, the entropic term becomes vanishingly small and the miscibility becomes increasingly dependent on the contribution of the enthalpic term. To enhance the formation of a miscible one-phase system in polymer blends, it is necessary to ensure that favorable specific intermolecular interactions exist between two base components of the blend. Many attempts have been made to decrease the interfacial energy and reduce the propensity for polymer blends to undergo phase separation, including the use of compatibilizers such as block and graft copolymers. Another approach involves introducing functional groups to connect individual polymer main chains together non-covalently. Ideally, one polymer chain would possess donor sites and the other acceptor sites for hydrogen bonding, dipole–dipole, and/or π–π interactions [2–7]. The miscibility of an immiscible blend can be enhanced by introducing a functional group to one component to enable the formation of intermolecular interactions with another [8].

In previous studies [9,10] of the roles of intermolecular association in miscibility enhancement, we found that the incorporation of a small number of hydrogen bond acceptors or donors into a polystyrene chain renders the modified polymer miscible with phenolic resin (a well-known hydrogen bonding donor) [9] or poly(ε-caprolactone) (a well-known hydrogen bonding acceptor) [10], respectively. In addition to hydrogen bonding, π–π interactions also play an important role in enhancing the polymer miscibility in classic systems such as the PPO/PS blend.

The aim of this study was to extend the specific interactions within polymer blend systems to include both hydrogen bonding and π–π interactions. Poly(vinyl phenyl ketone) (PVPK) is an amorphous material that is used as a component of clear and pigmented lacquers. Unlike poly(methyl methacrylate) (PMMA) [11], PVPK possesses both acceptor groups (C=O) for hydrogen bonding and aromatic rings for π–π interactions with poly(vinyl phenol) (PVPh). Generalized two-dimensional (2D) correlation spectroscopy has recently been applied widely in polymer science [12–15]. This novel method allows the specific interactions between polymer chains to be investigated by treating the spectral fluctuations as a function of time, temperature, pressure, and composition. 2D-IR correlation spectroscopy can identify different intra- and intermolecular interactions through the analysis of selected bands from the 1D vibration spectrum. The aims of this study were (1) to investigate blends of PVPK and the PS-*co*-PVPh copolymer, (2) to use 1D and 2D Fourier transform infrared (FTIR) spectroscopy to provide evidence for specific intermolecular association, and (3) to use the Painter–Coleman association model (PCAM) to predict whether a miscibility window exists for PVPK/PS-*co*-PVPh blends [16].

2. Experimental

2.1. Materials

PVPK (weight-average molecular weight: ca. 5900 g/mol) was obtained from Scientific Polymer Products. It is difficult to

* Tel.: +886 7 5252000x4079; fax: +886 7 5254099.
E-mail address: kuosw@faculty.nsysu.edu.tw

0032-3861/$ – see front matter © 2008 Elsevier Ltd. All rights reserved.
doi:10.1016/j.polymer.2008.08.002

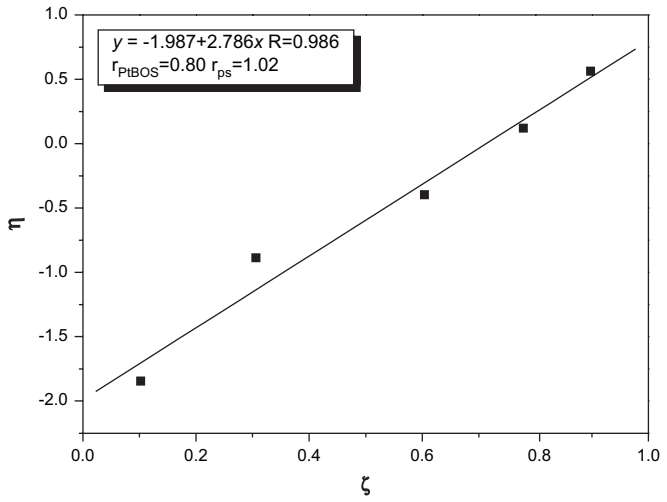

Fig. 1. Kelen–Tudos plot for PS-*co*-PtBOS copolymers.

synthesize poly(vinyl phenol) through direct polymerization of vinyl phenol because of the occurrence of side reactions involving the OH group during polymerization. As a result, the poly(styrene-*co*-vinyl phenol) copolymers were synthesized through copolymerization of styrene and 4-*tert*-butoxystyrene. The monomer reactivity ratios [r_1 (styrene) = 1.02; r_2 (4-*tert*-butoxystyrene) = 0.80] were determined (Fig. 1) using the methodology of Kelen and Tudos [17,18]; several copolymers containing various contents of 4-*tert*-butoxystyrene were obtained [19]. The solution copolymerization of styrene with 4-*tert*-butoxystyrene in benzene was performed at 70 °C under an argon atmosphere within glass reaction flasks equipped with condensers. AIBN was employed as the initiator; the mixtures were stirred for ca. 24 h. To determine the reactivity ratios, samples of the copolymers were taken from the reaction flasks during the early stages of copolymerization, i.e., when the degrees of conversion were low (4–9%). The copolymers were purified through a process of repeated precipitation in methanol/water (3:7, v/v) from THF solutions. The synthesized poly(styrene-*co*-4-*tert*-butoxystyrene) (PS-*co*-PtBOS) was dissolved in dioxane at a concentration of 10% (w/v). The solution was then heated under reflux overnight in the presence of 37% HCl to remove the *tert*-butoxy groups. Before vacuum drying, the poly(styrene-*co*-vinyl phenol) (PS-*co*-PVPh or PSOH) was precipitated repeatedly from THF solution into methanol/water and then purified through Soxhlet extraction with water for 72 h to remove any residual HCl. The copolymers were characterized using nuclear magnetic resonance (NMR) and FTIR spectroscopy, differential scanning calorimetry (DSC), and gel permeation chromatography (GPC). Table 1 lists the monomer feed ratios and resultant copolymer compositions of the PSOH copolymers.

Table 1
Characteristics of the poly(styrene-*co*-vinyl phenol) samples

Copolymer	Phenol ratio (mol%)[a]	Abb. name	M_n[b]	M_w/M_n[b]	T_g (°C)	T_d[c] (°C)
PS	0	PS	8000	1.21	90	371
PVPh5-*r*-PS95	4.6	PSOH5	22,000	2.03	101	370
PVPh22-*r*-PS78	21.5	PSOH22	24,000	2.05	104	368
PVPh36-*r*-PS64	36.0	PSOH36	17,400	2.05	118	365
PVPh55-*r*-PS45	55.2	PSOH55	23,200	2.10	154	359
PVPh78-*r*-PS22	77.8	PSOH78	24,400	2.34	162	353
PVPh	100	PVPh	20,000	1.07	175	352

[a] Obtained from ^{1}H NMR spectrum.
[b] Obtained through GPC analysis.
[c] The 5 wt% loss decomposition temperature.

2.2. Blend preparation

Blends of PSOH/PVPK were prepared through solution blending. THF solutions containing 5 wt% of the polymer mixture were stirred for 6–8 h; the solvent was then left to evaporate slowly at room temperature for 24 h. The blend films were then dried at 50 °C for 2 days.

2.3. Characterization

Molecular weights and molecular weight distributions were determined at 35 °C through GPC using a Waters 510 HPLC equipped with a 410 differential refractometer, a UV detector, and three Ultrastyragel columns (100, 500, and 10^3 Å) connected in series; THF was the eluent; the flow rate was 0.6 mL/min. The molecular weight calibration curve was obtained using polystyrene standards. ^{1}H and ^{13}C NMR spectra were obtained using an INOVA 500 instrument; acetone-d_6 was the solvent. The glass transition temperatures (T_g) of the polymer blend films were determined through DSC using a TA Q-20 instrument. The scan rate was 20 °C/min within the temperature range 30–200 °C; the temperature was then held at 200 °C for 3 min to ensure complete removal of residual solvent. The T_g measurements were performed in the DSC sample cell after the sample (5–10 mg) had been cooled rapidly to −50 °C from the melt of the first scan. The glass transition temperature was defined at the midpoint of the heat capacity transition between the upper and lower points of deviation from the extrapolated liquid and glass lines. FTIR spectra of the polymer blend films were recorded using the conventional KBr disk method. A THF solution containing the blend was cast onto a KBr disk and dried under conditions similar to those used in the bulk preparation. The film used in this study was sufficiently thin to obey the Beer–Lambert law. FTIR spectra were recorded using a Bruker Tensor 27 FT-IR spectrophotometer; 32 scans were collected at a spectral resolution 1 cm^{-1}. Because polymers containing OH groups are hygroscopic, pure nitrogen gas was used to purge the spectrometer's optical box to maintain the sample films' dryness. Generalized 2D correlation analysis was performed using the 2D Shige software developed by Shigeaki Morita (Kwansei-Gakuin University, Japan). In the 2D correlation maps, white-colored regions are defined as positive correlation intensities; shaded regions are defined as negative correlation intensities.

3. Results and discussion

3.1. Analyses of PVPh/PVPK blends

DSC analysis is one of the most convenient methods available to determine the miscibility of polymer blends. Fig. 2 displays the DSC thermograms of PVPh/PVPK blends of various compositions; each of the PVPh/PVPK blends possesses a single glass transition temperature, strongly suggesting that they are fully miscible blends exhibiting a homogeneous amorphous phase. Over the years, a number of equations have been offered to predict the variation of the glass transition temperature of a miscible blend as a function of composition. The most popular equation is the Kwei equation [20]:

$$T_g = \frac{W_1 T_{g1} + kW_2 T_{g2}}{W_1 + kW_2} + qW_1 W_2 \quad (1)$$

where W_1 and W_2 are the weight fractions of the components, T_{g1} and T_{g2} represent the corresponding glass transition temperatures, and k and q are fitting constants. Fig. 3 presents a plot of the dependence of the value of T_g on the composition of the miscible PVPh/PVPK blends; values of k and q of 1 and −60 were obtained from the non-linear least-squares "best fit." The parameter q

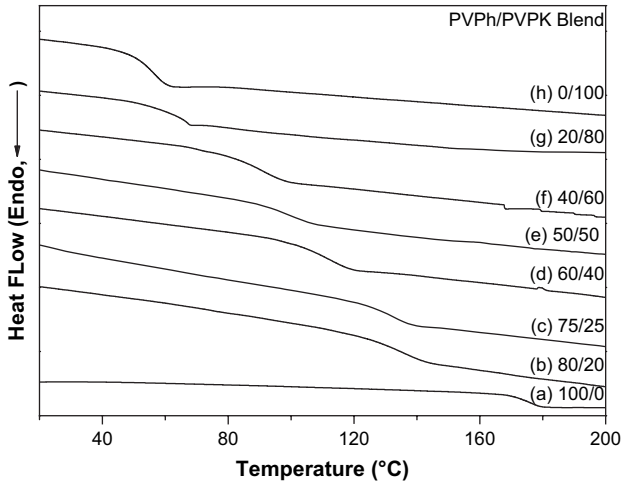

Fig. 2. DSC thermograms of various PVPh/PVPK blends.

corresponds to the strength of hydrogen bonding in the blend, reflecting a balance between the breaking of self-associative and the forming of inter-associative hydrogen bonds. The negative value of q indicates that intermolecular hydrogen bonding was weaker than the intramolecular hydrogen bonding.

Fig. 4 displays partial FTIR spectra (from 1630 to 1720 cm^{-1}) recorded at 25 °C for various PVPh/PVPK blend compositions. The C═O stretching frequency appears split into two bands at 1680 and 1660 cm^{-1}, corresponding to free and the hydrogen-bonded C═O

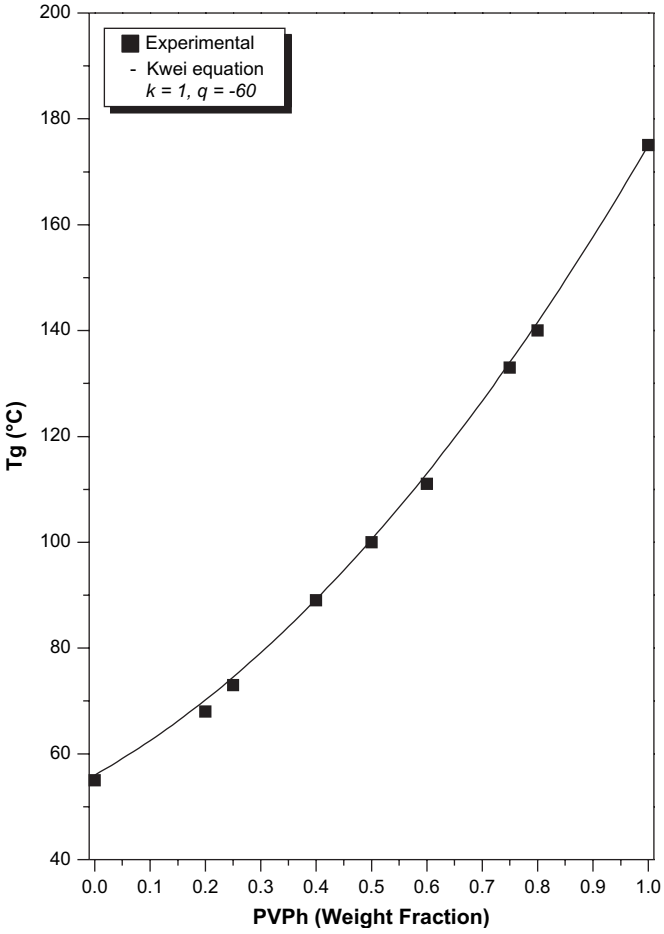

Fig. 3. Plots of T_g with respect to composition, based on (■) experimental data and (–) the Kwei equation.

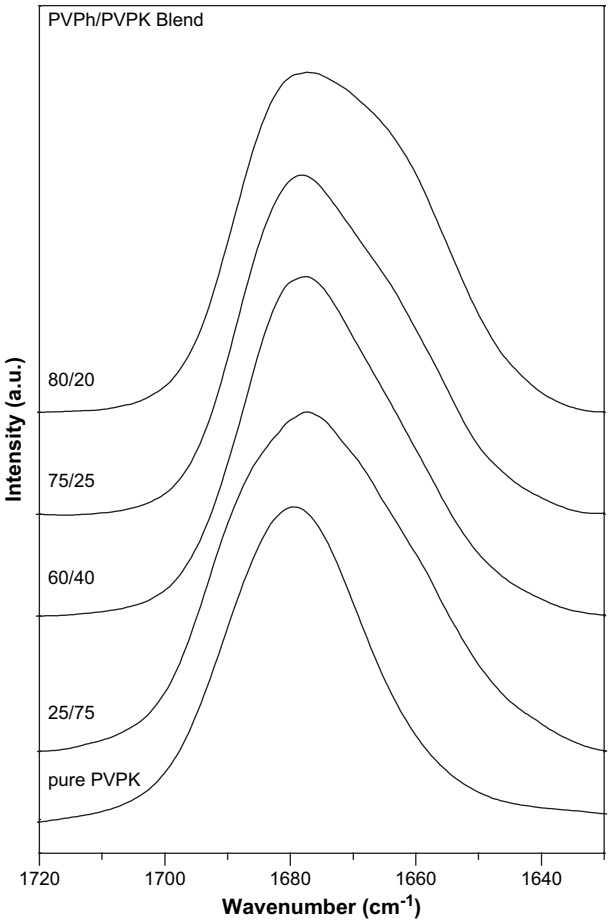

Fig. 4. Partial room-temperature FTIR spectra (1630–1720 cm^{-1}) of various PVPh/PVPK blends.

groups, respectively. The fraction of hydrogen-bonded C═O groups increased upon increasing the PVPh content. The bands were readily decomposed into two Gaussian peaks to determine the areas of the signals corresponding to the hydrogen-bonded (1660 cm^{-1}) and free (1680 cm^{-1}) C═O groups. The relative fractions of free and hydrogen-bonded C═O groups were calculated using an absorptivity coefficient of 1.5, i.e., the ratio of the intensity of the two bands [16]. Table 2 summarizes the spectral parameters for the C═O bands, and reveals that fraction of hydrogen-bonded C═O groups of PVPK increased upon increasing the PVPh content.

Fig. 5 displays partial FTIR spectra (OH stretching region; 2700–4000 cm^{-1}) of pure PVPh, pure PVPK, and various PVPh/PVPK blends. The pure PVPh exhibits two bands in the OH stretching region: a very broad band centered at 3350 cm^{-1}, attributed to the wide distribution of the hydrogen-bonded OH groups, and a narrower shoulder band at 3525 cm^{-1}, representing free OH groups. The intensity of free OH absorption (3525 cm^{-1}) decreased

Table 2
Parameters obtained after curve fitting room-temperature FTIR spectra of PVPh/PVPK blends

PVPh/PVPK	Hydrogen-bonded C═O			Free C═O			f_b
	ν, cm^{-1}	$W_{1/2}$, cm^{-1}	A_b, %	ν, cm^{-1}	$W_{1/2}$, cm^{-1}	A_b, %	
Pure PVPK	–	–	–	1680	24.8	100	0
25/75	1662	21.7	20.0	1680	23.5	80.0	14.28
40/60	1662	20.3	26.3	1680	21.3	73.7	18.97
60/40	1662	20.4	33.1	1680	21.4	66.9	24.71
75/25	1662	20.6	38.1	1680	21.1	61.9	29.25
80/20	1662	20.5	41.3	1680	21.5	58.7	31.89

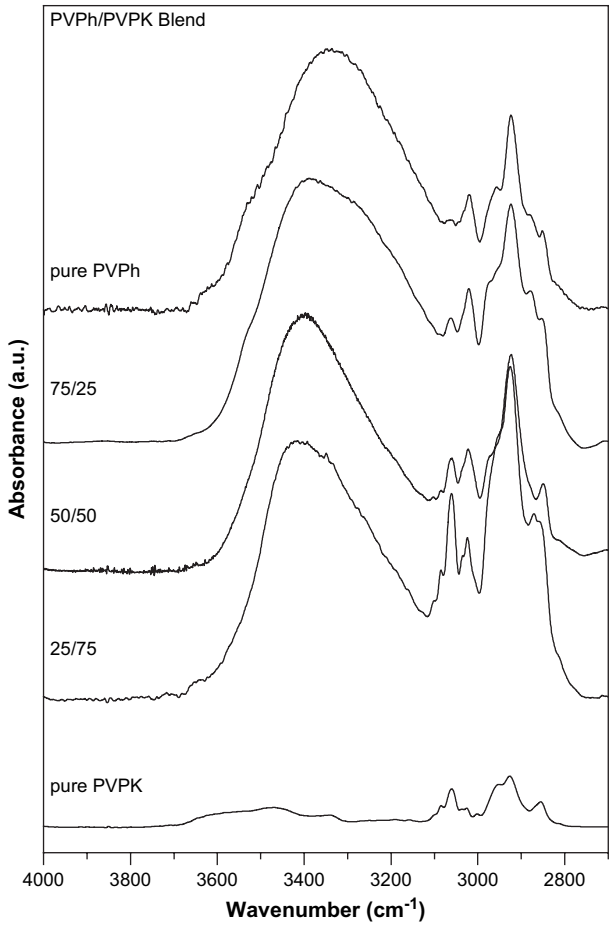

Fig. 5. Partial room-temperature FTIR spectra (2700–4000 cm^{-1}) of various PVPh/PVPK blends.

gradually as the PVPK content of the blend was increased from 25 to 75 wt%. The band for the hydrogen-bonded OH groups in the phenolic shifted to higher frequency (toward 3420 cm^{-1}) upon increasing the PVPK content. This phenomenon resulted from a switch from OH···OH to OH···O=C hydrogen bonds. Therefore, it is reasonable to assign the band at 3420 cm^{-1} to the signal of the OH groups that were hydrogen-bonded to C=O groups. The frequency difference between the free and the hydrogen-bonded OH groups can be used to determine the average strength of the intermolecular interactions [16]. In this study, OH···O=C inter-association ($\Delta\nu = 105\ cm^{-1}$) was weaker than the self-association of the OH groups of the phenolic ($\Delta\nu = 175\ cm^{-1}$), consistent with the negative value of q determined from the Kwei equation.

3.2. Inter-association equilibrium constant of PVPh/PVPK blend

Fig. 6 provides a plot of the fraction of hydrogen-bonded C=O groups of PVPK versus the PVPh weight fraction in the two-blend system. The PCAM [16] can be used to determine the equilibrium constants describing self-association and inter-association and other thermodynamic properties. The self-association equilibrium constants, K_2 and K_B, corresponding to the OH···OH interactions of phenolic, represent the formation of hydrogen-bonded "dimers" and "multimers," respectively. In this study, a suitable value for K_A of 10 for the PVPh/PVPK blend was based on the experimental data and theoretical predictions. The calculation of the inter-association equilibrium constants using the least-squares method has been discussed previously [21]. Table 3 lists all of the parameters required by the PCAM to estimate the thermodynamic properties of

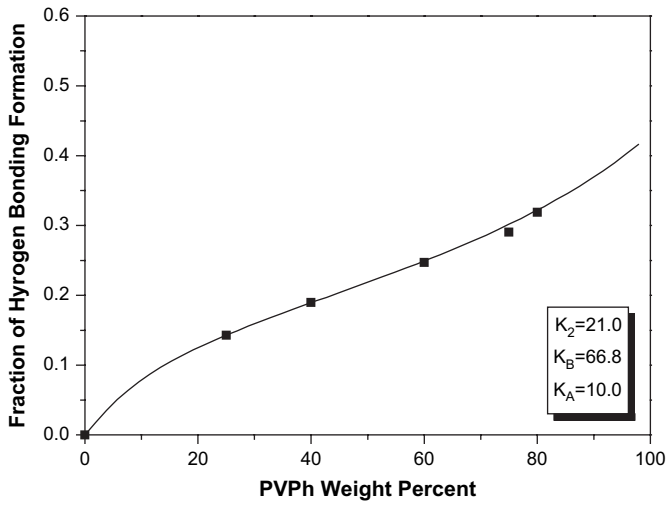

Fig. 6. Plot of the fraction of the hydrogen-bonded C=O groups with respect to composition: (■) FTIR spectral data; (–) theoretical values for polymer blends calculated at 25 °C.

these polymer blends. Clearly, the inter-association equilibrium constant of PVPh/PVPK is weaker than the self-association equilibrium constant of pure PVPh, which results in the negative value of q.

3.3. Two-dimensional correlation analysis of PVPh/PVPK blends

White and shaded areas in 2D-IR correlation contour maps represent positive and negative cross-peaks, respectively. 2D-IR correlation spectra are characterized by two independent wavenumber axes and a correlation intensity axis. In general, two types of spectra, 2D synchronous and asynchronous, are obtained; the correlation intensities in the 2D synchronous and asynchronous maps reflect the relative degrees of in-phase and out-of-phase responses, respectively. The 2D synchronous spectra are symmetric with respect to the diagonal line in the correlation map. Auto peaks, which represent the degree of autocorrelation of perturbation-induced molecular vibrations, are located at the diagonal positions of a synchronous 2D spectrum; their values are always positive. When an auto peak appears, the signal at that wavenumber would change greatly under environmental perturbation. Cross-peaks located at off-diagonal positions of a synchronous 2D spectrum (they may be positive or negative) represent the simultaneous or coincidental changes of the spectral intensity variations measured at ν_1 and ν_2. Positive cross-peaks result when the intensity variations of the two peaks at ν_1 and ν_2 occur in the same direction (i.e., both increase or both decrease) under the environmental perturbation; negative cross-peaks reveal that the intensities of the two peaks at ν_1 and ν_2 change in opposite directions (i.e., one increases while the other decreases) under perturbation [22].

Table 3
Self-association and inter-association equilibrium constants and thermodynamic parameters for PVPh/PVPK blends at 25 °C

Polymer	V	MW	δ	DP	Equilibrium constants		
					K_2	K_B	K_A
PVPh[a]	100.0	120.0	10.6	160	21.0	66.8	–
PVPK[a]	104.6	132.1	11.0	45	–	–	10

V: Molar volume (mL/mol); MW: molecular weight (g/mol); δ: solubility parameter $(cal/mL)^{1/2}$; DP: degree of polymerization; K_2: dimer self-association equilibrium constant; K_B: multimer self-association equilibrium constant; K_A: inter-association equilibrium constant.

[a] Ref. [16].

As in the case for a synchronous spectrum, the sign of an asynchronous cross-peak can be either negative or positive, providing useful information on the sequential order of events observed by the spectroscopic technique along the external variable. The 2D asynchronous spectra are asymmetric with respect to the diagonal line in the correlation map. According to Noda's rule [22], when $\Phi(\nu_1,\nu_2) > 0$, if $\psi(\nu_1,\nu_2)$ is positive (black colored area), band ν_1 will vary prior to band ν_2; if $\psi(\nu_1,\nu_2)$ is negative (white-colored area), band ν_2 will vary prior to band ν_1. This rule is reversed, however, when $\Phi(\nu_1,\nu_2) < 0$. In summary, if the symbols of the cross-peak in the synchronous and asynchronous maps are the same (both positive or both negative), band ν_1 will vary prior to band ν_2; if the symbols of the cross-peak are different in the synchronous and asynchronous spectra (one positive and the other negative), band ν_1 will vary after ν_2 under the environmental perturbation.

Fig. 7(a) presents the synchronous 2D correlation maps in the range 1500–1700 cm^{-1}. Absorption bands in this spectral range that are associated with PVPh appear at 1612, 1595, and 1510 cm^{-1}, corresponding to an in-plane C–C stretching frequency of a ring influenced by an OH group (phenyl-OH), the in-plane C–H stretching vibration of a ring influenced by an OH group, and another in-plane C–C stretching frequency of a ring influenced by an OH group (phenyl-OH), respectively; (cf. those of pure polystyrene at 1601, 1583, and 1493 cm^{-1}, respectively). Signals associated with PVPK appear at 1680, 1595, and 1580 cm^{-1}, which are attributable to vibration of the free C═O groups, in-plane C–C stretching of rings, and in-plane C–H stretching of rings, respectively. Clear, positive cross-peaks existed between the signal at 1680 cm^{-1} and those at 1612 and 1510 cm^{-1}, implying the existence of hydrogen bonding between free C═O groups of PVPK (1680 cm^{-1}) and phenol-OH groups (1612 and 1510 cm^{-1}) of PVPh. The positive cross-peaks at 1680, 1612, and 1510 cm^{-1} all exhibit the same direction according to Noda's rule. Fig. 7 also reveals a positive cross-peak between the signals at 1612 and 1580 cm^{-1}, revealing the presence of π–π interactions between aromatic rings of PVPh and PVPK; these two cross-peaks occur in the same direction (both increase or both decrease). Thus, the specific interactions between PVPh and PVPK arise not only from hydrogen bonding but also from π–π interactions. The fraction of hydrogen-bonded C═O groups and the inter-association equilibrium constant of PVPh/PVPK are both significantly lower than those of the PVPh/PMMA blend system, implying that the phenol-OH groups of PVPh may also interact with PVPK through π–π interactions.

Fig. 7(b) displays the asynchronous 2D correlation maps in the range 1500–1700 cm^{-1}. The auto peak at 1680 cm^{-1} splits into the two separate bands for PVPK located at ca. 1680 and 1660 cm^{-1}. This phenomenon suggests that there are two different C═O group sites in PVPK. One, at the relatively lower wavenumber (1660 cm^{-1}), represents C═O groups involved in hydrogen bonding interactions with the OH groups of PVPh; the other, at higher wavenumber (1680 cm^{-1}), represents free C═O groups. This result is similar to the findings in the 1D FTIR spectra in Fig. 4. Furthermore, the cross-peaks between the signal at 1680 cm^{-1} and those at 1612 and 1510 cm^{-1} and between the signals at 1612 and 1580 cm^{-1} in Fig. 7(b) exhibit opposing intensity orders, indicating that these two bands result from different polymer chains, i.e., intermolecular hydrogen bonding or π–π interactions. In addition, the positive peaks at 1612, 1680 cm^{-1}, 1680, 1580 cm^{-1}, and 1612, 1580 cm^{-1} in the asynchronous map of Fig. 7(b) imply that the intensity of the peak at 1612 cm^{-1} alters before that at 1680 cm^{-1}, 1680 cm^{-1} alters before that at 1580 cm^{-1}, and 1612 cm^{-1} alters before that at 1580 cm^{-1} upon increasing the PVPh content. In total, the 2D map reveals that the sequence of changing intensity of the three bands observed in the spectra is $1612 > 1680 > 1580\ cm^{-1}$.

Fig. 8 provides an analysis of the 1550–1720 and 3000–3600 cm^{-1} regions, which represent the signals for OH stretching bands, to provide a macroscopic view of the interactions. The sign of the cross-peaks at 1680, 3400 cm^{-1} is negative in both the synchronous [Fig. 8(a)] and asynchronous [(b)] maps. Thus, we infer that the changes in intensity of these bands occur in the opposite direction, according to Noda's rule (one decreases, the other increases), meaning that the intensity of the signal for the free C═O group of PVPK will decrease upon increasing the OH group content of PVPh; we also infer that the change in the intensity of the signal at 1680 cm^{-1} is greater than that at 3400 cm^{-1} upon increasing the PVPh content. In addition, the signs of the cross-peaks at 1660, 3400 cm^{-1} and 1612, 3400 cm^{-1} are positive in both the synchronous [Fig. 8(a)] and asynchronous [(b)] maps. Thus, we infer that these changes in intensity occur in the same direction according to Noda's rule (i.e., both decrease or both increase), which means that the signal for the hydrogen-bonded C═O group of PVPK will increase in intensity upon increasing the OH group content of PVPh. Taken together, the 2D analyses in Figs. 7 and 8 suggest that the

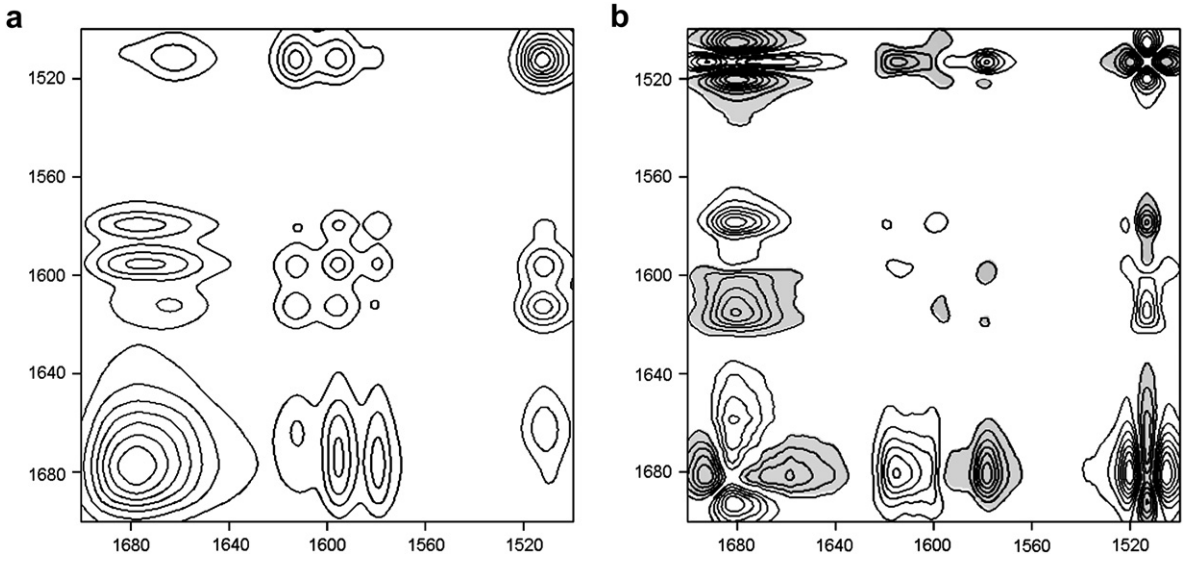

Fig. 7. (a) Synchronous and (b) asynchronous 2D correlation maps for the region from 1500 to 1700 cm^{-1}.

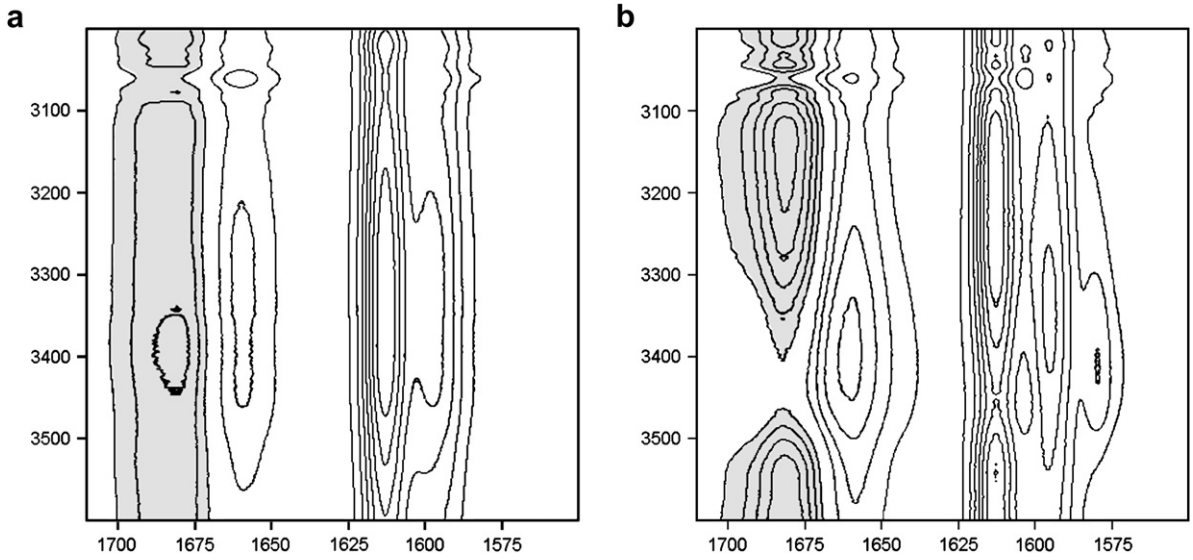

Fig. 8. (a) Synchronous and (b) asynchronous 2D correlation maps for the regions from 1500 to 1700 cm^{-1} and from 3000 to 3600 cm^{-1}.

sequence of intensity increases is 1612 > 1680 > 1660 > 3400 cm^{-1}. Furthermore, no cross-peak is evident at 1580, 3400 cm^{-1}, indicating the OH groups of PVPh do not interact with the aromatic rings of PVPK. Thus, it appears that the phenyl-OH groups initially form hydrogen bonds with the free C=O groups of PVPK, consistent with the signal for the OH groups initially shifting to higher wavenumber upon increasing the PVPK content (Fig. 4). In the second step, the phenyl-OH groups interact with the aromatic rings of PVPK through π–π interactions. Finally, the phenyl-OH groups of PVPh interact with the OH groups of PVPh.

3.4. Analyses of PS-co-PVPh/PVPK blend

The glass transition behavior of PVPK blended with the various amounts of PS-*co*-PVPh was examined using DSC. Fig. 9 displays typical results for selected PS-*co*-PVPh contents over a wide range of PVPh levels. Table 4 summarizes whether one or two T_g values were noted for all PS-*co*-PVPh/PVPK = 50/50 blends. Clearly, blends of PVPK with PS-*co*-PVPh copolymers containing 20 mol% or more of PVPh exhibited a single glass transition, indicating complete miscibility within this window of PVPh contents. Fig. 10 presents partial FTIR spectra (1630–1720 cm^{-1}) measured at 25 °C for PS-*co*-PVPh/PVPK = 50/50 blends containing various amounts of PVPh in the PS-*co*-PVPh copolymers. Similar to the situation in the spectra in Fig. 4, the C=O stretching bands of these blends are split into two signals, i.e., those for absorptions of free and hydrogen-bonded C=O groups at 1680 and 1660 cm^{-1}, respectively. Quantitative analyses of these C=O bands provides a direct measure of the degree of mixing in these polymer blends. The fraction of hydrogen-bonded C=O groups increased upon increasing the PVPh content in the PS-*co*-PVPh copolymer. Therefore, the blend containing a higher PVPh content in the PS-*co*-PVPh copolymer forms a greater number of hydrogen bonds, thereby forming a one-phase

Table 4
DSC thermograms of PS-*co*-PVPh/PVPK = 50/50 for various PVPh contents

Compositions	T_g		
PS/PVPK	46		88
PSOH5/PVPK	63		98
PSOH22/PVPK		88	
PSOH36/PVPK		95	
PSOH55/PVPK		101	
PSOH78/PVPK		107	
PVPh/PVPK		110	

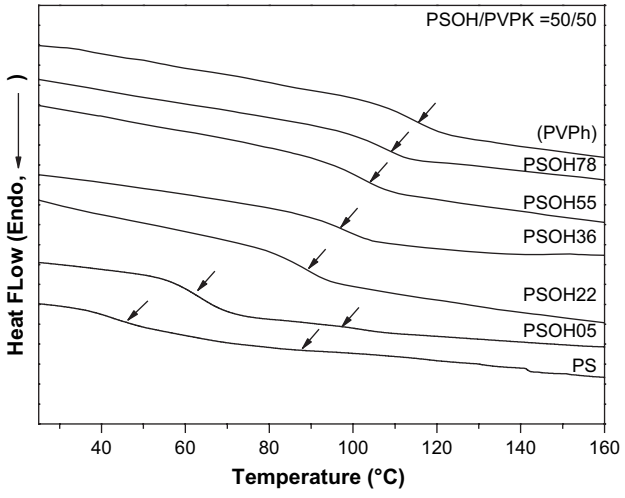

Fig. 9. DSC curves of PSOH/PVPK = 50/50 blends containing various amounts of PVPh.

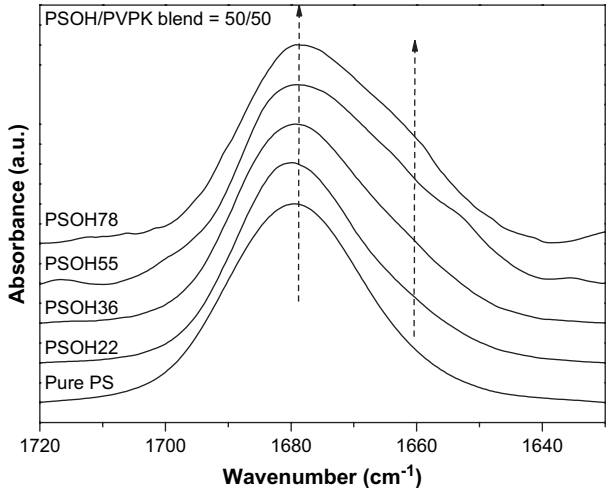

Fig. 10. Partial FTIR spectra (1630–1720 cm^{-1}) of PSOH/PVPK = 50/50 blends containing various amounts of PVPh.

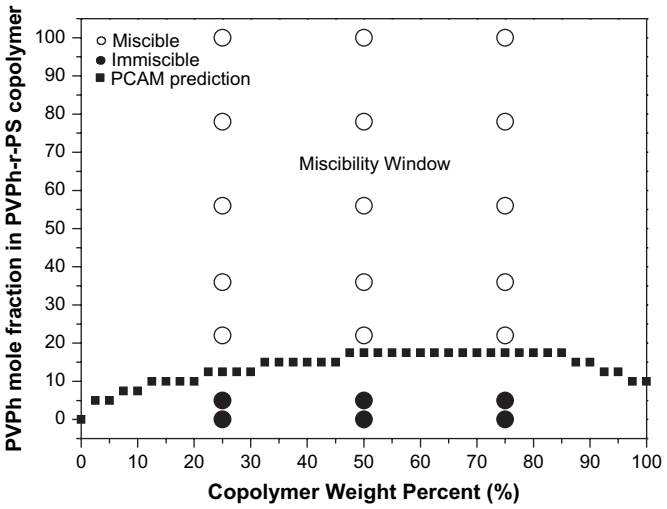

Fig. 11. Theoretical miscibility windows for phenolic/PS-*co*-PAS blends obtained from the Painter–Coleman association model (▲) spinodal curve and experimental data: (●) two-phase system; (○) one-phase system.

system more preferably. The presence of a significant fraction of hydrogen bonds may result in a well-mixed system, but it does not necessarily imply the existence of a thermodynamically miscible blend. Fortunately, we can use the Painter–Coleman association model to calculate and define the miscibility window, taking advantage of the known molar volumes, molecular weights, solubility parameters, degrees of polymerization, and equilibrium constants (including self-association and inter-association) in Table 3.

3.4.1. Miscibility window prediction

Painter and Coleman [23] suggested adding an additional term – accounting for the free energy of hydrogen bond formation – to a simple Flory–Huggins expression for the free energy of mixing of two polymers:

$$\frac{\Delta G_N}{RT} = \frac{\Phi_1}{N_1}\ln\Phi_1 + \frac{\Phi_2}{N_2}\ln\Phi_2 + \Phi_1\Phi_2\chi_{12} + \frac{\Delta G_H}{RT} \quad (2)$$

where Φ and N are the volume fraction and the degree of polymerization, respectively, χ is the "physical" interaction parameter, and the subscripts 1 and 2 define the two-blend components. ΔG_H is the free energy change contributed by hydrogen bonding between two components, which can be estimated from the FTIR spectra. According to the Painter–Coleman equation (2), two major factors are responsible for this increase in the miscibility window. Firstly, when the difference in the solubility parameters of the two polymer components of the blend decreases, the value of χ will decrease. Therefore, incorporation of PVPh (10.29 cal/cm^3) units into PS will decrease the difference between the solubility parameters of PS (9.48 cal/cm^3) and PVPK (11.0 cal/cm^3) [23]. Secondly, the relative strength of inter-association over self-association increases upon increasing the PVPh content in the PS-*co*-PVPh copolymer, tending to enhance the favorable contribution from the ΔG_H/RT term in Eq. (2) and thereby result in a favorable trend for miscibility. Fig. 11 displays the miscibility window for PS-*co*-PVPh/PVPK blends at 180 °C as predicted theoretically using the PCAM [23]. We choose this temperature to compare the theoretical and experimental data because it is above the glass transition temperature and because the DSC curves were obtained after quenching the sample from this temperature. Therefore, it is reasonable to calculate the miscibility window after quenching from 180 °C, where equilibrium conditions are retained. The *x*-axis in Fig. 11 represents the weight fraction of PS-*co*-PVPh in the blend; the *y*-axis represents the mole percentage of PVPh in the PS-*co*-PVPh copolymer. The plot suggests that PVPh will be completely miscible with PS-*co*-PVPh/PVPK blends when the PVPh content is greater than 20 mol%. Thus, the model's predicted miscibility window at 180 °C compares favorably with our experimental results based on DSC analyses.

4. Conclusions

The FTIR spectra revealed that the phenol units of PVPh interact strongly with the C=O groups of PVPK through intermolecular hydrogen bonding, and more weakly with the aromatic rings of PVPK through intermolecular π–π interactions. Incorporating vinyl phenol monomer into PS can enhance the miscibility of PS with PVPK because the value of χ decreases and the degree of inter-association increases between the C=O groups of PVPK and the OH groups of the PVPh units in the PS-*co*-PVPh copolymer. PVPK was miscible with PS-*co*-PVPh copolymers having vinyl phenol contents greater than 20 mol%. The Painter–Coleman association model predicts the miscibility of this blend system well.

Acknowledgment

This work was supported financially by the National Science Council, Taiwan, Republic of China, under Contract No. NSC-96-2120-M-009-009 and NSC-96-2218-E-110-008.

References

[1] Park P, Zimmerman SC. J Am Chem Soc 2006;128:11582.
[2] Kuo SW, Chang FC. Macromolecules 2001;34:5224.
[3] Kuo SW, Chang FC. Macromolecules 2001;34:4089.
[4] Kuo SW, Huang WJ, Huang CF, Chan SC, Chang FC. Macromolecules 2004;37:4164.
[5] Wang J, Cheung MK, Mi Y. Polymer 2001;42:2077.
[6] Li X, Goh SH, Lai YH, Wee ATS. Polymer 2000;41:6563.
[7] Cesteros LC, Isasi JR, Katime I. Macromolecules 1993;26:7256.
[8] Chien YY, Perace EM, Kwei TK. Macromolecules 1988;21:1616.
[9] Kuo SW, Chang FC. Polymer 2001;42:9843.
[10] Kuo SW, Chang FC. Macromolecules 2001;34:7737.
[11] Kuo SW, Huang CF, Tung PH, Huang WJ, Huang JM, Chang FC. Polymer 2005;46:9348.
[12] Lin CL, Chen WC, Liao CS, Su YC, Huang CF, Kuo SW, et al. Macromolecules 2005;38:6435.
[13] Noda I. J Am Chem Soc 1989;111:8116.
[14] Lee YJ, Kuo SW, Huang WJ, Lee HY, Chang FC. J Polym Sci Polym Phys Ed 2004;42:1127.
[15] Kuo SW, Lin HC, Huang WJ, Huang CF, Chang FC. J Polym Sci, Polym Phys Ed 2006;44:673.
[16] Coleman MM, Gref JF, Painter PC. Specific interactions and the miscibility of polymer blends. Lancaster, PA: Technomic Publishing; 1991.
[17] Kennedy JP, Kelen T, Tudos F. J Polym Sci Polym Chem Ed 1975;13:2277.
[18] Kelen T, Tudos FF. Macromol Sci Chem (A) 1975;9:1.
[19] Lin HC, Wang CF, Kuo SW, Tung PH, Lin CH, Chang FC. J Phys Chem B 2007;111:3404.
[20] Kwei TK. J Polym Sci Polym Lett Ed 1984;22:307.
[21] Kuo SW, Chang FC. Macromol Chem Phys 2001;202:3112.
[22] Noda I, Ozaki Y. Two-dimensional correlation spectroscopy. John Wiley & Sons; 2004.
[23] Coleman MM, Painter PC. Miscible polymer blend-background and guide for calculations and design. DEStech Publications, Inc; 2006.